Number4 Volume13 December 2007 Journal of Engineering

NUMERICAL INVESTIGATION OF NATURAL CONVECTION IN A VERTICAL ANNULUS ENCLOSURE

Ass. Prof. Manal H. AL-Hafidh
University of Baghdad
Mechanical Eng. Dept

Safa Bontok Raheem
University of Baghdad
Mechanical Eng. Dept

ABSTRACT

A numerical technique is developed to predict both the transient and steady axisymmetric two-dimensional natural convection heat transfer for water as the working fluid in a vertical annulus enclosure of a fixed radius ratio (2) aspect ratio (1) and Rayleigh number ranging within ($10^3 \leq Ra_d \leq 10^6$) for a fixed Prandtl number (Pr=7). Finite difference analogs of the Navier – Stokes and thermal energy equations are solved in the stream function – vorticity frame work. The results obtained are presented graphically in the form of streamline, vorticity and isotherm contour plots. A correlation has been set up to give the average Nusselt number variation with Ra_d and for which the results are found to be in good agreement with previously published experimental data.

الخلاصة

يتضمن البحث دراسة رقمية باستخدام طريقة الفروق المحددة لدراسة انتقال الطاقة الحرارية بالحمل الحر لماء في حيّز حلقي عمودي ثنائي البعد لأسطوانتين متمركزتين مغلقتي النهايات ولنسبة أقطار ثابتة(٢) لنسبة باعية As] [$(r_o - r_i)$ /ι= تساوي (١) وخواص جريان ($10^3 \leq Ra_d \leq 10^6$) و(Pr=7). تم حل معادلات الاستمرارية والزخم والطاقة الانتقالية بعد تحليلها إلى معادلات لا بعدية ومن ثَمّ إلى دالّة الانسياب الدوّاميّة. النتائج تم توضيحها برسم منحنيات مغلقة للانسياب ومنحنيات درجات الحرارة الثابتة، والنتائج أعطت تمثيلاً لمعدل رقم نسلت ($\tilde{N}u_i$) ضد Ra_d. المقارنة مع البحوث الأخرى أعطت نتائج دقيقة كفاية لإمكانية حساب معامل انتقال الطاقة الحرارية لحالة الجريان المذكورة آنفاً وللماء كوسط لانتقال الحرارة .

KEY WORDS: Natural Convection, Concentric Vertical Annulus, Laminar Flow, Numerical Solution

INTRODUCTION

The annulus represents a common geometry employed in a variety of heat transfer systems ranging from simple heat exchangers to the most complicated nuclear reactors. In spite of the importance of convection heat transfer in vertical annular enclosures in many practical applications, very few basic studies have so far been conducted for this system. Many finite difference solutions of free convection problems of long horizontal, rectangular and cylindrical enclosures subject to lateral heating are found in the works of **(Boyd, 1983), (Charrier-Mojtabi and Mojtabi et-al, 1979), (Date, 1986), (Kuhen & Golstein, 1976) and (Akbar et-al, 1985).** Numerical studies of free convection in vertical annulus enclosures are found in the works of **(Schwab & De Witt, 1970), (Kubair & Simha, 1982) (Keyhani et-al, 1983) and (Prasad & Kulacki, 1985)**. Many investigators interested in the study of eccentric annular enclosures **(Shue et-al, 2001)** or elliptic cylinders **(Lee and Lee, 1981).** Most of the studies available are for high aspect ratio.

The present paper considers the axisymmetric flow regime in a vertical annulus enclosure **Fig. (1)** whose surface temperatures are kept isothermal and with Boussinesq approximation being made to the governing equations.

MATHEMATICAL FORMULATION

The problem considered are both the transient and steady state, two-dimensional axisymmetric laminar convection of a Boussinesq fluid initially at rest and a uniform temperature is assumed in the mathematical model for the system shown in **Fig. (1).** The vertical cylindrical surfaces are considered to be perfect conductors of heat with the inner wall temperature (Ti) greater than that of the outer wall (To). Both top and bottom surfaces of the enclosure are considered to be perfect insulators with a rigid and motionless bounding surfaces. The dimensionless equations of continuity, momentum and energy are **(Schwab & De Witt, 1970)**:

$$(^1/_R)[R\,(\partial U/\partial R)] + (\partial V/\partial Z) = 0 \quad (1)$$

$$(\partial U/\partial T_M)+U(\partial U/\partial R)+V(\partial U/\partial Z) = -(\partial P/\partial R)+Pr[\partial/\partial R\{(^1/_R)(\partial RU/\partial R)\}+(\partial^2 V/\partial Z^2)] \quad (2)$$

$$(\partial V/\partial T_M)+V(\partial V/\partial R)+(\partial V/\partial Z) = -(\partial P/\partial Z)+Pr[(^1/_R)(\partial/\partial R\{R(\partial V/\partial R)\}+(\partial^2 V/\partial Z^2)] \quad (3)$$

$$(\partial \Theta/\partial T_M)+U\,(\partial \Theta/\partial R)+V(\partial \Theta/\partial Z) = (^1/_R)[(\partial/\partial R)\{R(\partial \Theta/\partial R)\}]+(\partial^2 \Theta/\partial Z^2) \quad (4)$$

The vorticity-stream function formulation is applied in order to avoid direct determination of the lateral variations of pressure. The conservation equations then become:

Vorticity:

$$(\partial \omega/\partial T_M) + (\partial U\omega/\partial R) + (\partial V\omega/\partial Z) = Ra_d\, Pr\,(\partial \Theta/\partial R) + Pr\,[(\partial/\partial R)\,\{(^1/_R)\,(\partial R\omega/\partial R)\} \quad (5)$$

Stream function:

$$\nabla^2\psi = -\omega = (^1/_R)\,[(\partial^2\psi/\partial R^2) - (^1/_R)\,(\partial\psi/\partial R) + (\partial^2\psi/\partial Z^2)] \quad (6)$$

Energy:

$$(^1/_R)(\partial RU\Theta/\partial R) + (\partial V\Theta/\partial Z) = (^1/_R)\,[(\partial/\partial R)\{R(\partial\Theta/\partial R)\}] + (\partial^2\Theta/\partial Z^2) \quad (7)$$

The initial and boundary conditions are:

For $T_M = 0$, $\omega = \psi = U = V = 0$ (no slip condition)

, $\Theta_i = 1$, $\Theta_o = 1$ (constant wall temperature)

For $T_M > 0$, $\psi = \partial\psi/\partial n = 0$, $\partial\Theta/\partial Z = 0$

$$\omega_{\text{Vertical wall}} = -(^1/_R)\,(\partial^2\psi/\,Z^2) \quad , \quad \omega_{\text{horizontal wall}} = -(^1/_Z)(\partial^2\psi/\,R^2)$$

NUMERICAL SOLUTION OF THE GOVERNING EQUATIONS

An analytic solution cannot be found for a set of equations because of the complexity of those characterizing the cavity problem, and thus they must be integrated numerically by finite difference techniques. In this study, the governing equations which are expressions of conservation of mass, momentum and thermal energy are non-dimensionalized. A two–dimensional explicit finite difference technique was used to solve the transient behavior of the fluid and the heat transfer until the steady state is reached by marching out in time step ΔT_M. A forward difference technique may used to convert the convection terms in the energy and vorticity transport equations to an algebraic terms and in concern of diffusion terms, the central difference technique may used. To get numerical stability, the forward difference technique is applied when the mean value of the velocity is positive and the backward difference technique is applied when the mean velocity value is negative, so the method choice depends on the flow direction. To solve the stream function equation the Gauss Siedel method used with the successive over relaxation method to make earlier convergence. A numerical stability occurred when the time step ΔT_M is greater than $(\Delta T_M)_{max.}$, which depends on Ra_d and grid spacing. In this study the suitable ΔT_M was found to be ($\Delta T_M \leq 0.0001$) for fixed Ra_d.
The main steps of the solution procedure can be listed as follow:

1. The boundary and initial conditions are specified for the dependent variables.
2. The discretized temperature equation is solved to obtain the updated temperature field.
3. Vorticity at all interior grid points was similarly advanced from using the updated temperature field.
4. Stream function at all interior grid points was updated with the updated vorticity field.
5. Local Nusselt number computed and the method of successive over relaxation was employed to obtain the new stream function at each grid point. Convergence was assumed whenever any two successive iterations was less than 10^{-4}.

6. Total heat transfer calculated depending on local Nusselt number.
7. Steps (1-6) were repeated until the magnitude of the error ratio (ε) did not change by more than 10^{-4}.

RESULTS AND DISCUSSION

The difference equations of this study were solved on a digital computer using FORTRAN 95 program and the Tec Plot program used to plot the isotherm and streamline contours. The results are expressed in the transient region until reaching steady state where $\tilde{N}u_i$ will be constant with time.

Transient Results

Grid Spacing

The time steps used depend on Ra_d as shown in **Table (1)**, and the grid spacing which was found to give an adequate representation of the results for $Ra_d=10^3$ and 10^4 was (1/10) and for $Ra_d=10^5$ and 10^6 the grid spacing were (1/20) and (1/30) respectively.

Table (2) explain the best values for nodes number (N) in radial direction and (M) in vertical direction for ($10^3 \leq Ra_d \leq 10^6$).

Flow and Isotherm Patterns

Figs. (2-13) show typical results obtained for vertical annuli with Rayleigh number ($10^3 \leq Ra_d \leq 10^6$), for different time steps. The fluid near the outer (colder) cylinder is heavier and is moving downward while the relatively lighter fluid near the inner (hotter) cylinder is moving upward and with the increase of Ra_d a slightly vertical displaced occurred towards the top of the annulus so the convection regime appears clearly as shown in **Figs. (2, 3, 4 and 5).**

The temperature gradient across the cavity is horizontal with conduction profiles being vertical lines traversing the entire length of the cavity as indicated in **Fig.(6)** and then start to develop and indicate more inclination in its lines while the slope of lines near (cold wall) is small because the velocity is decreased **Fig.(7, 8 and 9)**. When Ra_d approaches 10^3, large temperature gradients grow near the vertical wall giving rise to the formation of thermal boundary layers and fluid velocities sufficient to form hydrodynamic boundary layer. A unicellular flow pattern is generated in the enclosure. It is noticed that the maximum heat transfer, indicated by closely spaced isotherms, is located at the top of the cavity for the outer cylinder and at the bottom for the inner one.

As a consequence of the symmetry and the continuity, the resulting fluid motion inside the half cavity consists of one rotating vortex as shown in **Fig. (10)** when the time increasing a multi small vorticity will be appeared

In **Figs. (11, 12 and 13)** it is seen that a small secondary vorticity appears in the bottom and become smaller with time increasing where a start of forming of a secondary vorticity near the outer cylinder will happened which will be grow with the increasing of fluid velocity.

Temperature Distribution and Local Nusselt Number

Fig. (14) shows the temperature variation versus Ra_d for a gap width (z = 0.5). In the thermal boundary layer adjacent to the outer cylinder, it is seen that the temperature gradient increases considerably and the trend is opposite near the inner cylinder. This is probably due to higher heat transfer by angular convection flow rather than radial one.

A correlation of ($\tilde{N}u_i$) with respect of Ra_d was set up which is given as:

$$\tilde{N}u_i = 0.4134 * Ra_d^{0.287} \quad (8)$$

Steady State Results

Heat transfer rate can be calculated at a steady state when the average Nusselt number ($\tilde{N}u_i$), reach a constant value with time as shown in **Fig. (15).**

Steady state streamlines and the isotherms for Ra_d ranging within (10^3- 10^6) are explained in **Fig. (16 a & b) and Fig.(17 a & b)** respectively and the vorticity lines are explained in **Fig.(18 a& b)** which shows the multi-cellular flow regime except at ($Ra_d > 10^5$), where single vorticity appears.

A reasonable agreement between the present work results and the previous researches are shown in **Fig. (19).**

Table (1) Time Steps used with different Ra_d

ΔTM	Ra_d
0.0001	10^3
0.0001	10^4
0.00005	10^5
0.00001	10^6

Table (2) Best Values for the Selected Node Number for Study Cases

Ra_d	N	M
10^3- 10^4	11	11
10^5	21	21
10^6	31	31

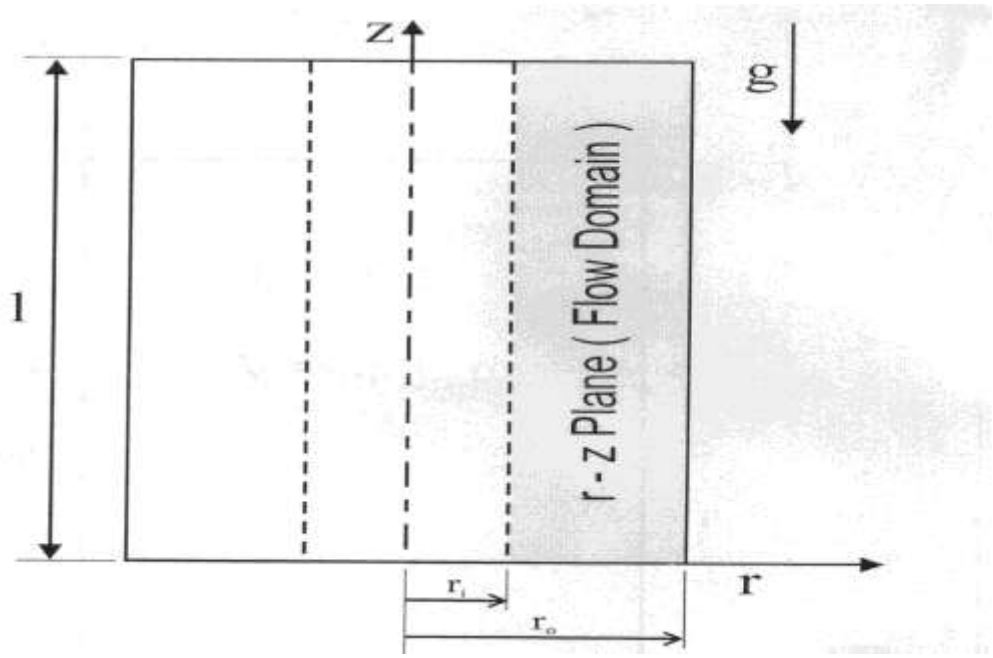

Fig. (1) Enclosure Geometry And Coordinate System

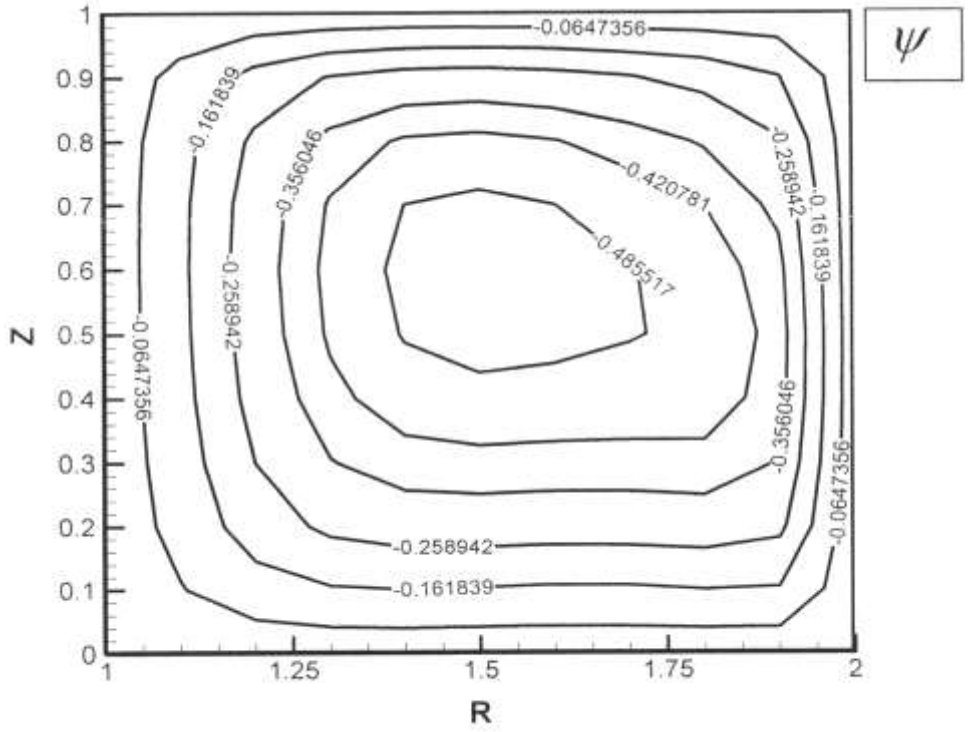

TM=0.056

Fig. (2) Transient Streamlines for $Ra_d = 10^3$

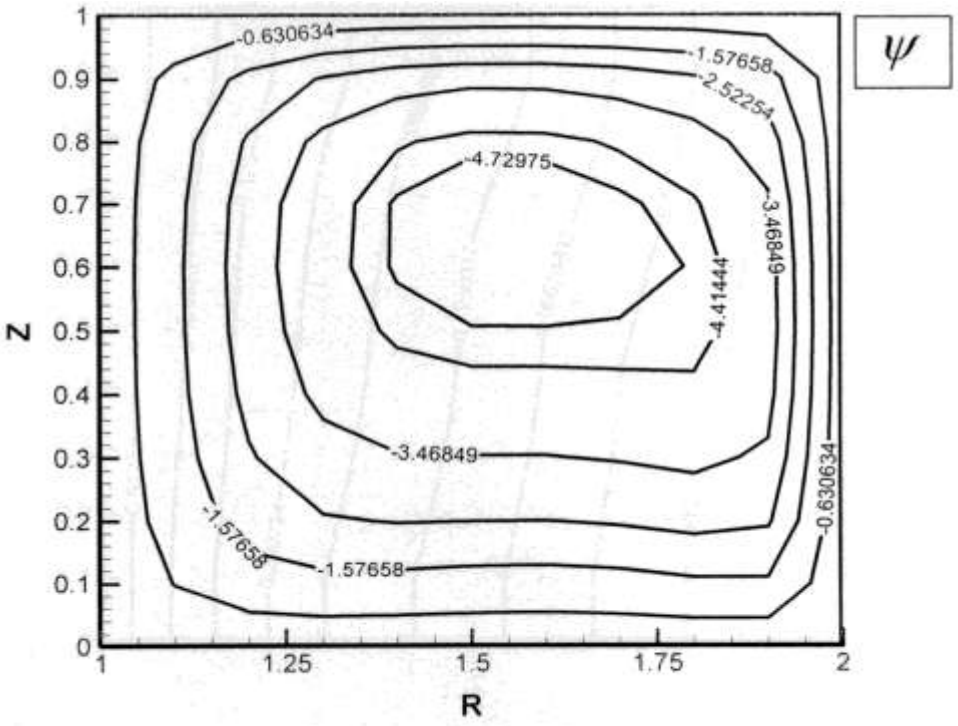

TM = 0.048

Fig. (3) Transient Streamlines for $Ra_d = 10^4$

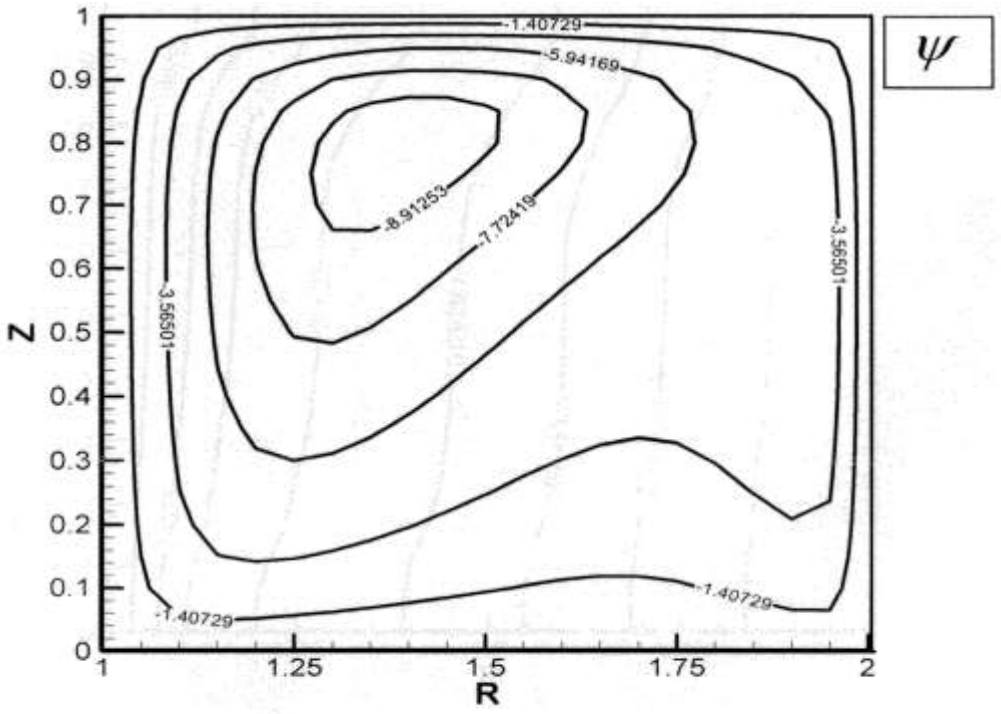

TM = 0.024

Fig. (4) Transient Streamlines for $Ra_d = 10^5$

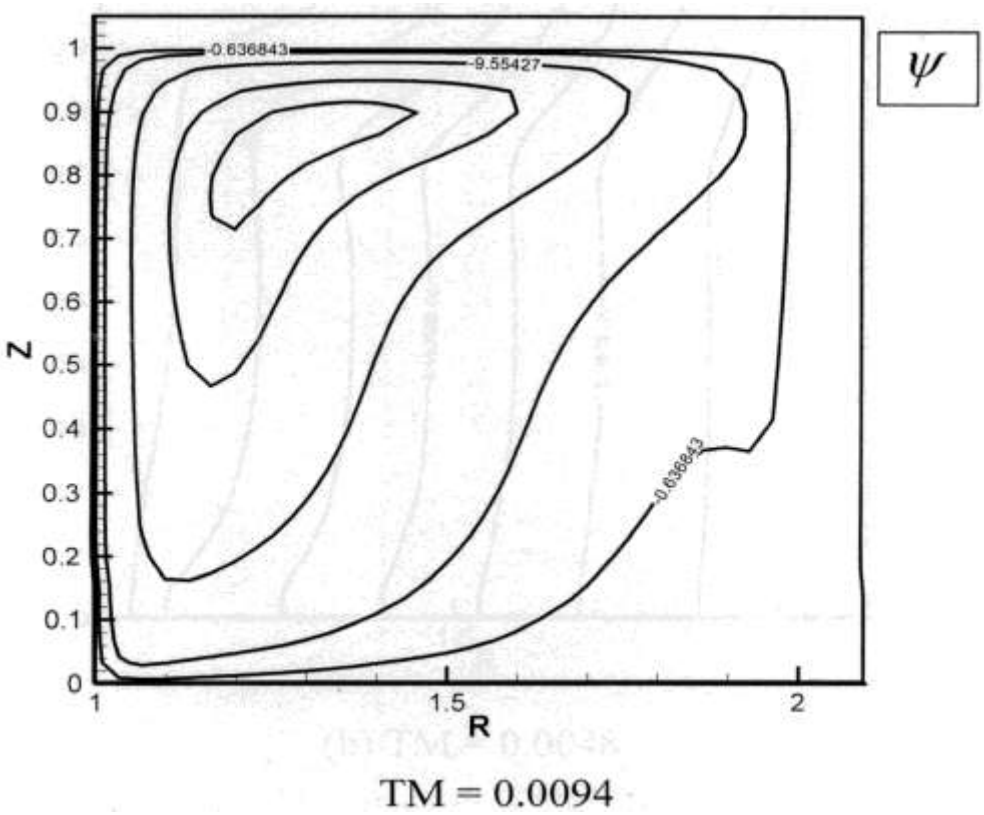

Fig. (5) Transient Streamlines for $Ra_d = 10^6$

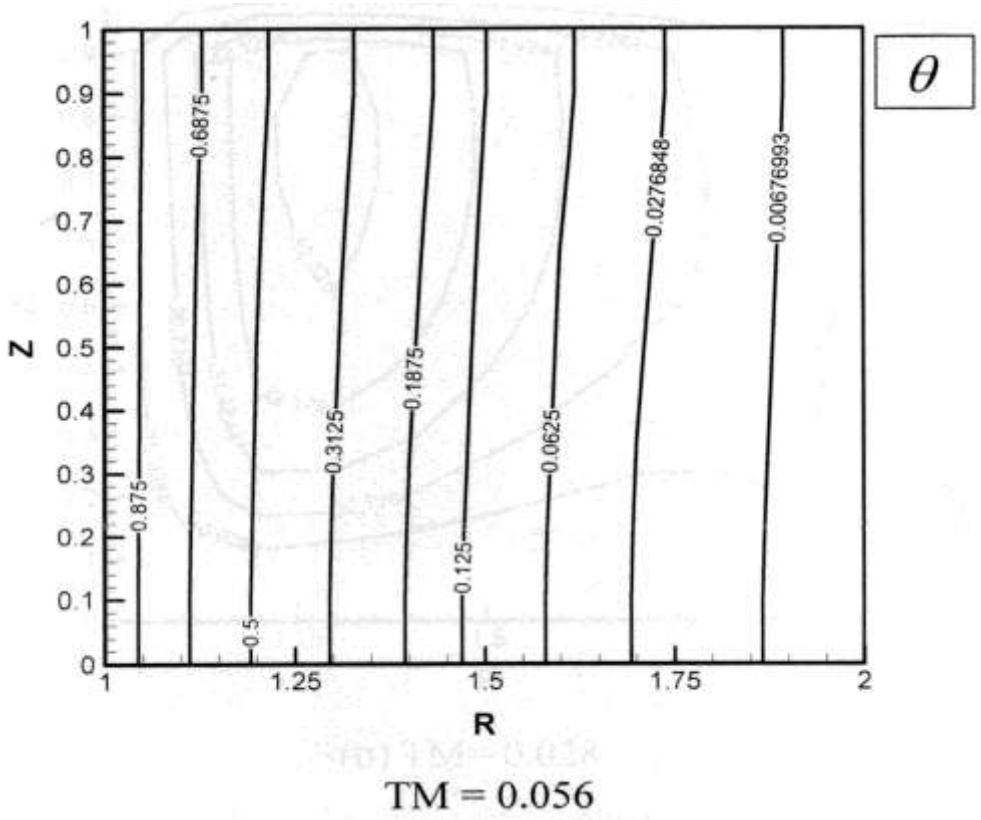

Fig. (6) Transient Isotherms for $Ra_d = 10^3$

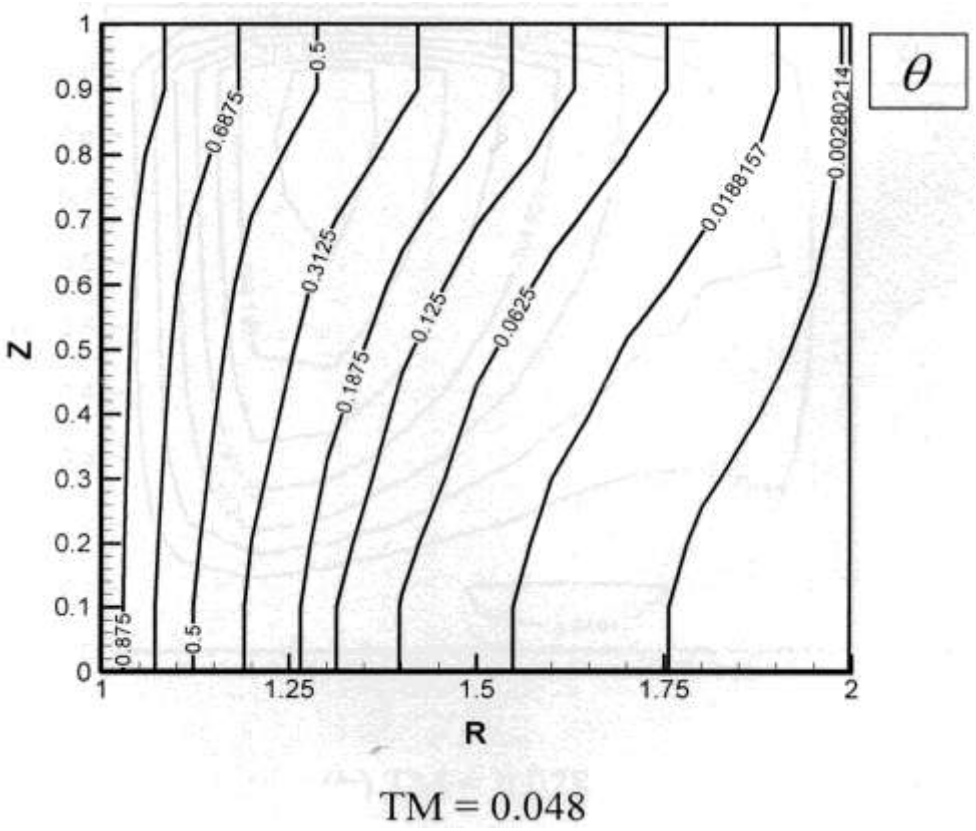

Fig. (7) Transient Isotherms for $Ra_d = 10^4$

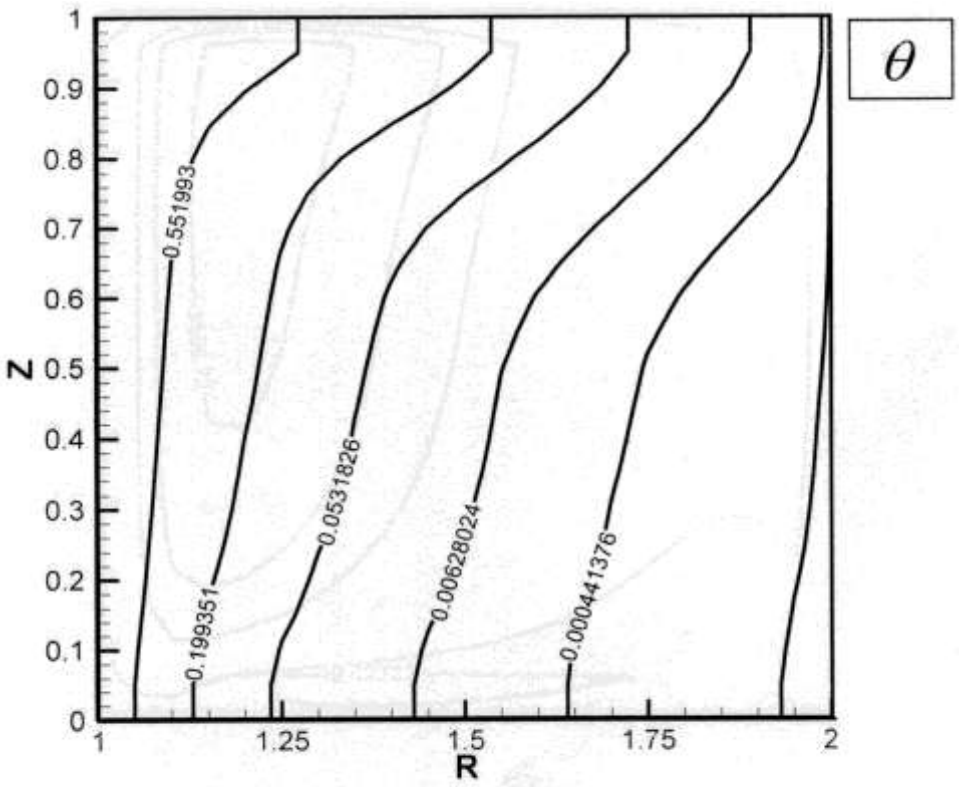

Fig. (8) Transient Isotherms for $Ra_d = 10^5$

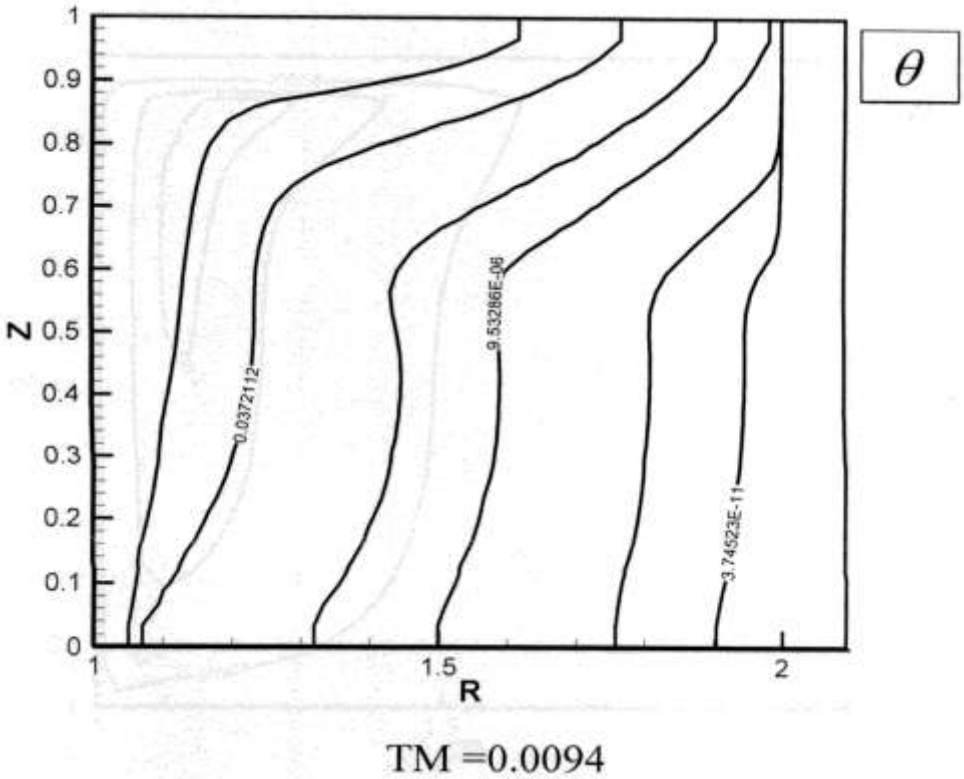

Fig. (9) Transient Isotherms for $Ra_d = 10^6$

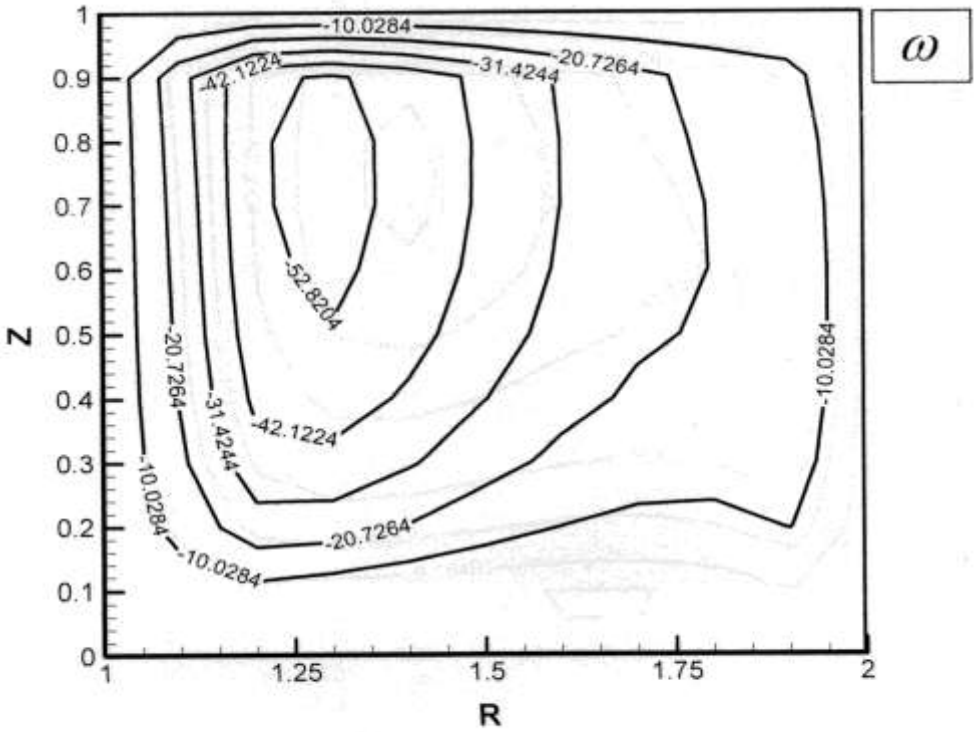

TM= 0.028

Fig. (10) Transient Vorticity for $Ra_d = 10^3$

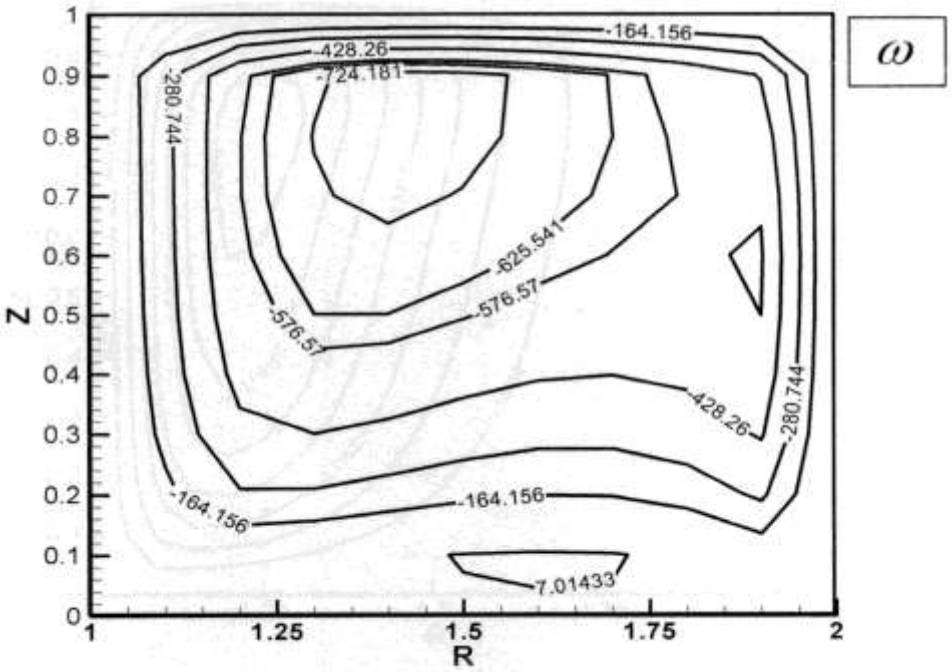

TM = 0.048

Fig. (11) Transient Vorticity for $Ra_d = 10^4$

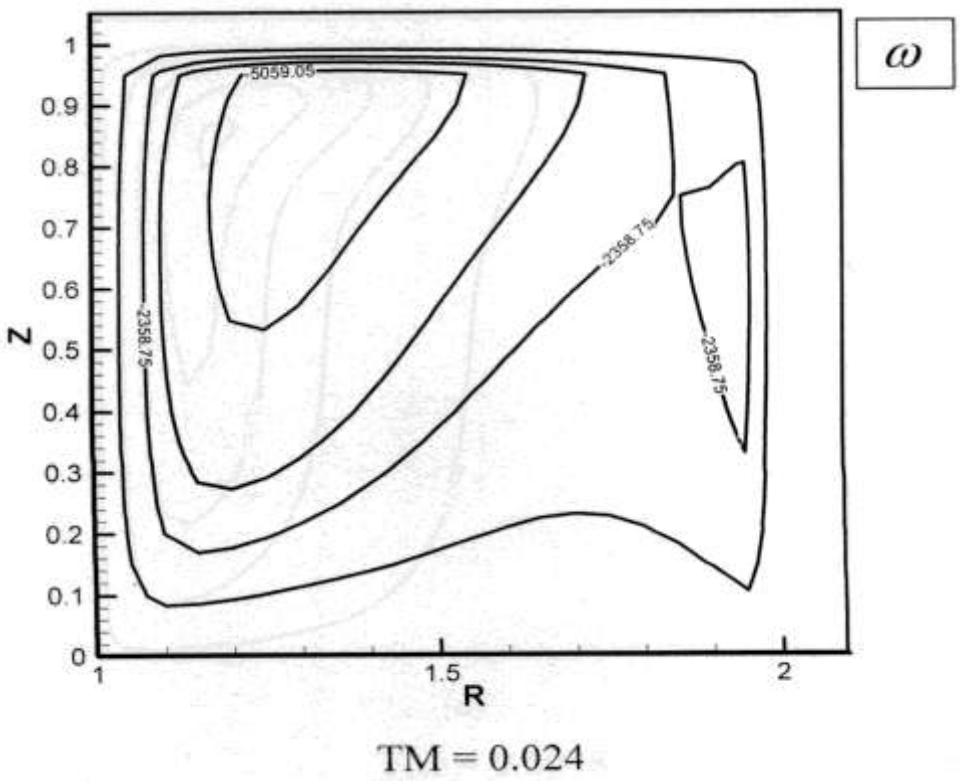

Fig. (12) Transient Vorticity for $Ra_d = 10^5$

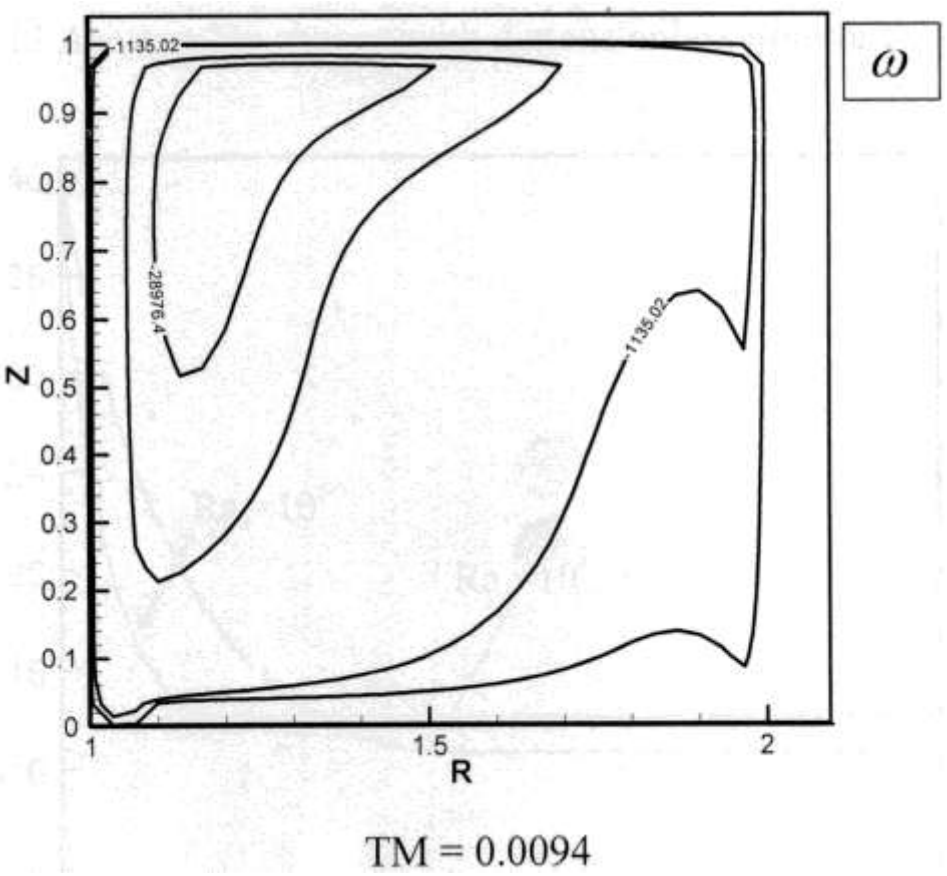

Fig. (13) Transient Vorticity for $Ra_d = 10^6$

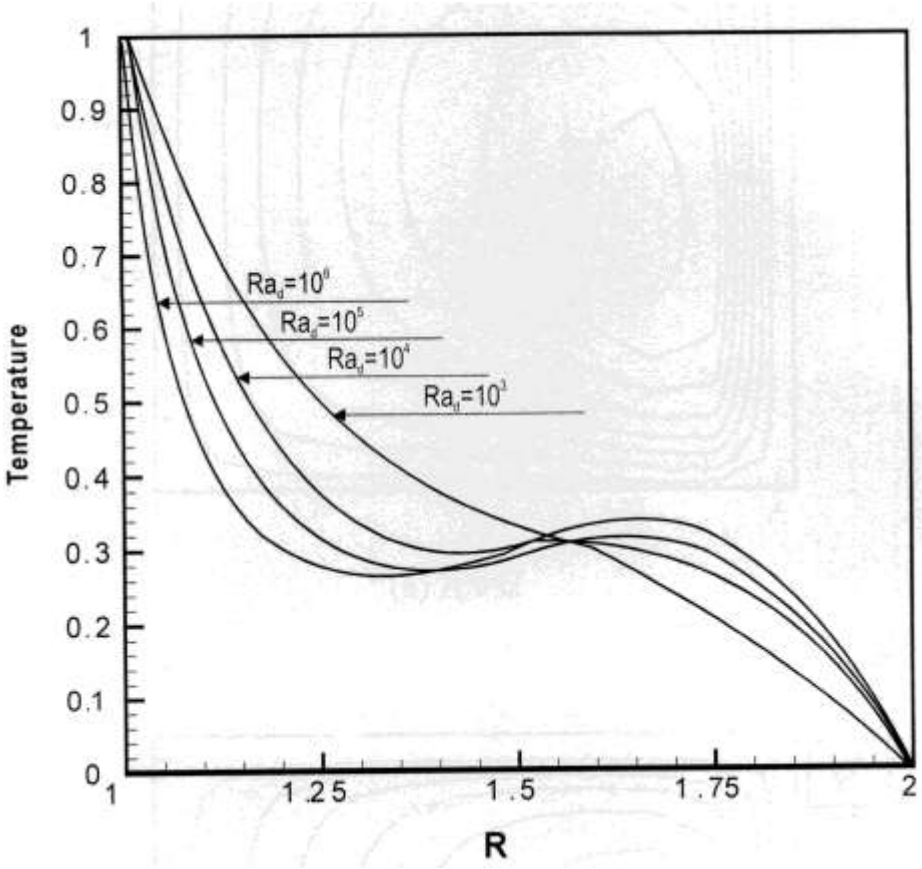

Fig. (14) Temperature Distribution with Gap Width at Z = 0.5

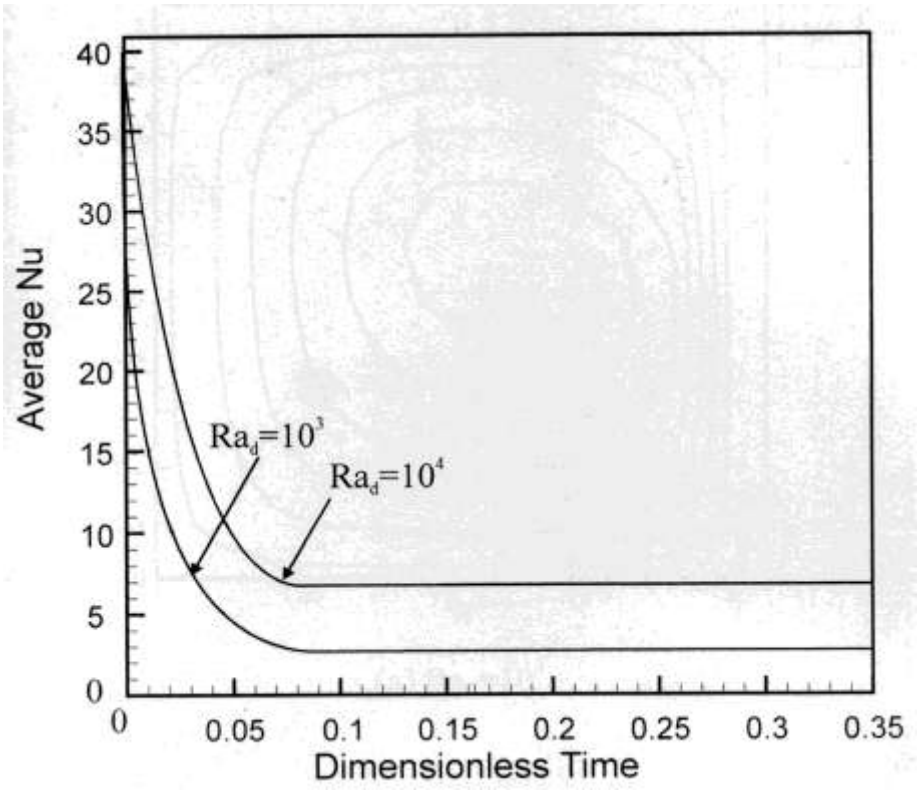

Fig. (15) Average Nu_i Change with Dimensionless Time for $Ra_d = 10^3$ & 10^4

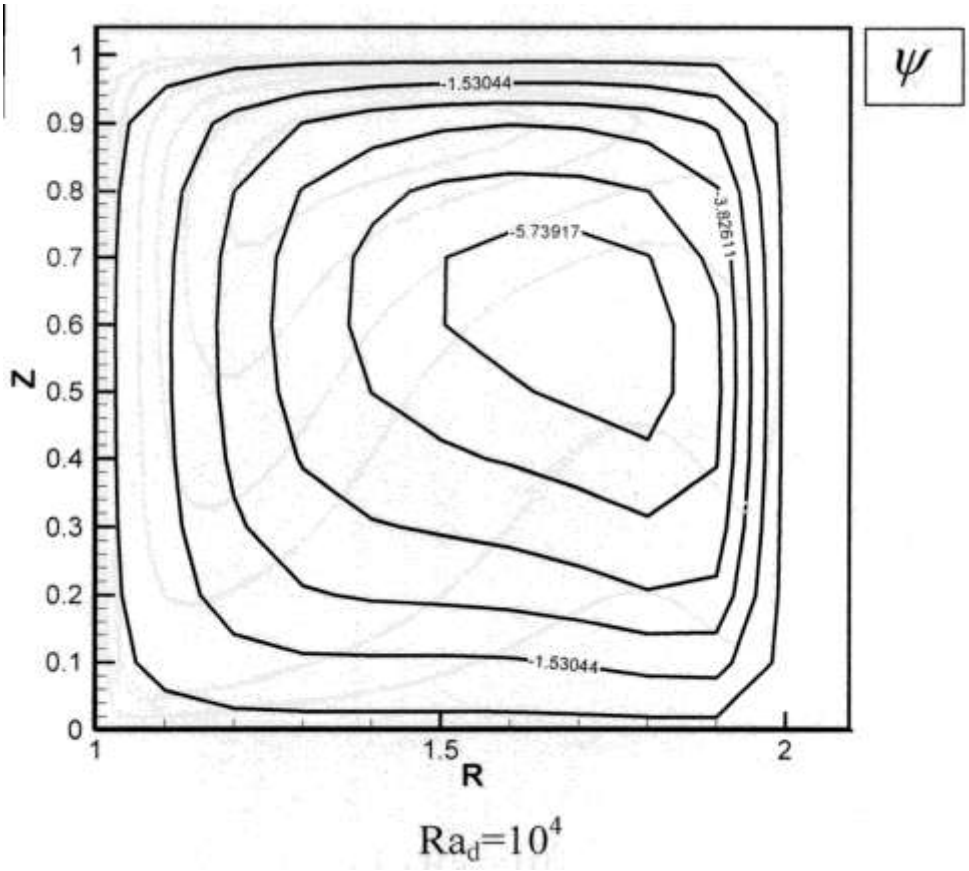

Fig. (16a) Steady State Streamlines for $Ra_d = 10^4$

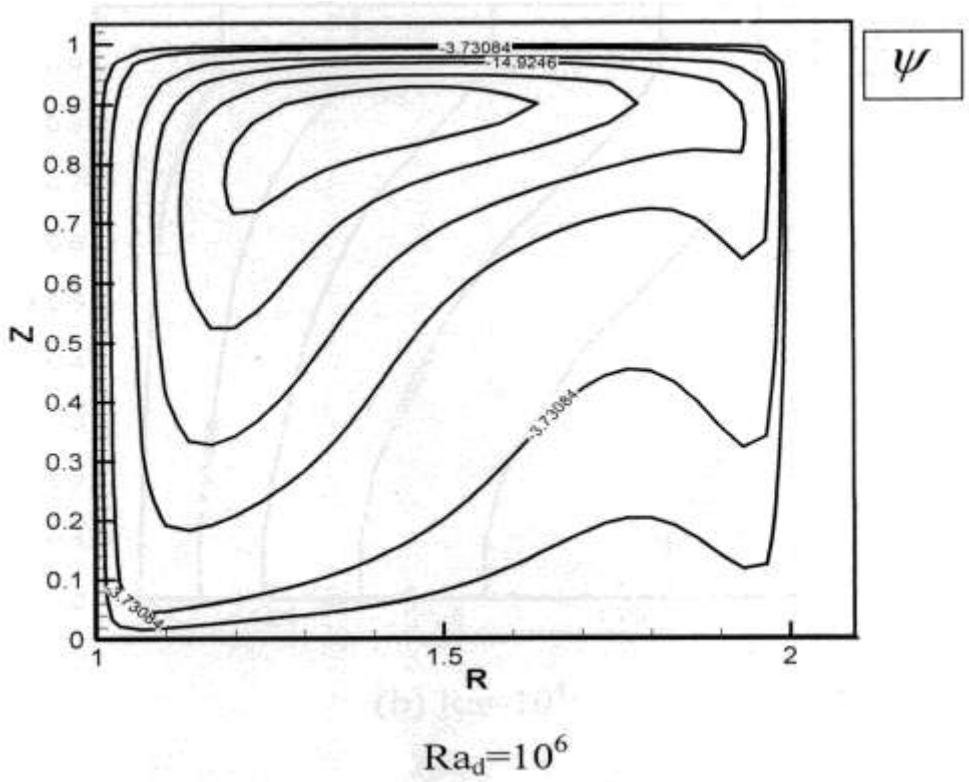

Fig. (16b) Steady State Streamlines for $Ra_d = 10^6$

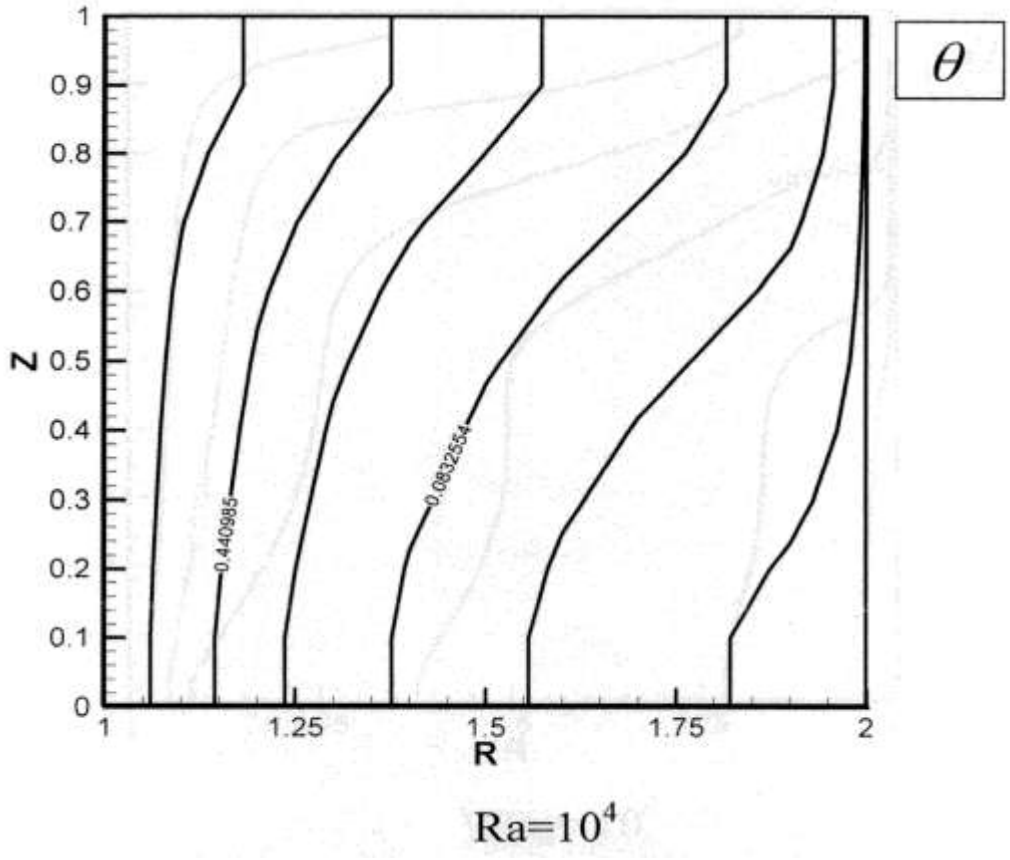

Fig. (17a) Steady State Isotherms for $Ra_d = 10^4$

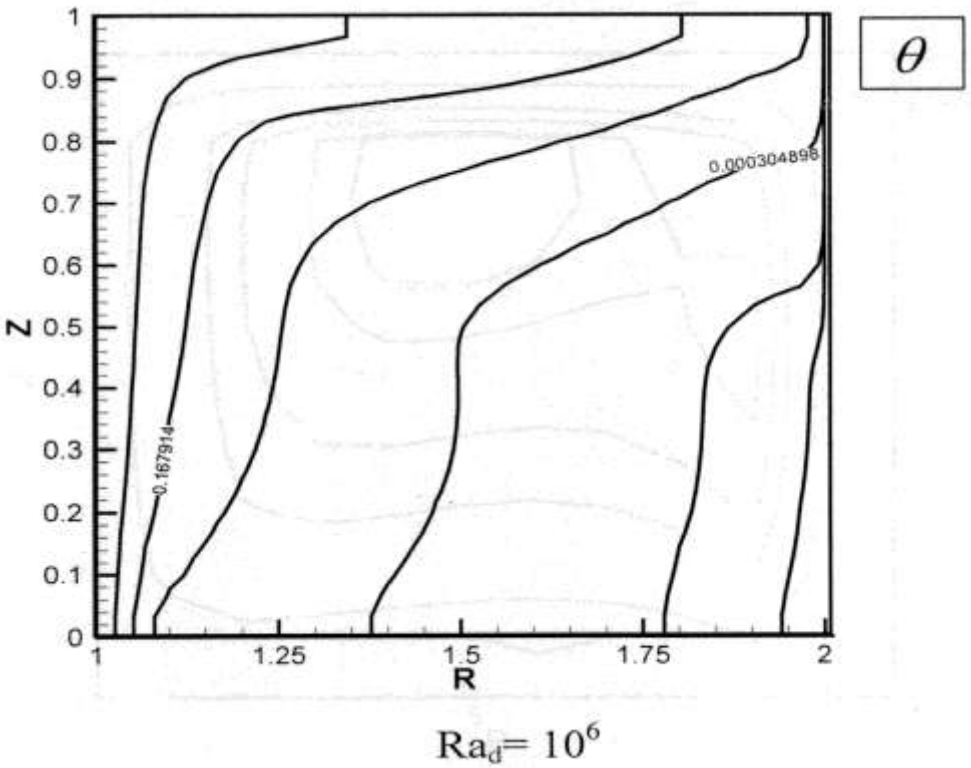

$Ra_d = 10^6$

Fig. (17b) Steady State Isotherms for $Ra_d = 10^6$

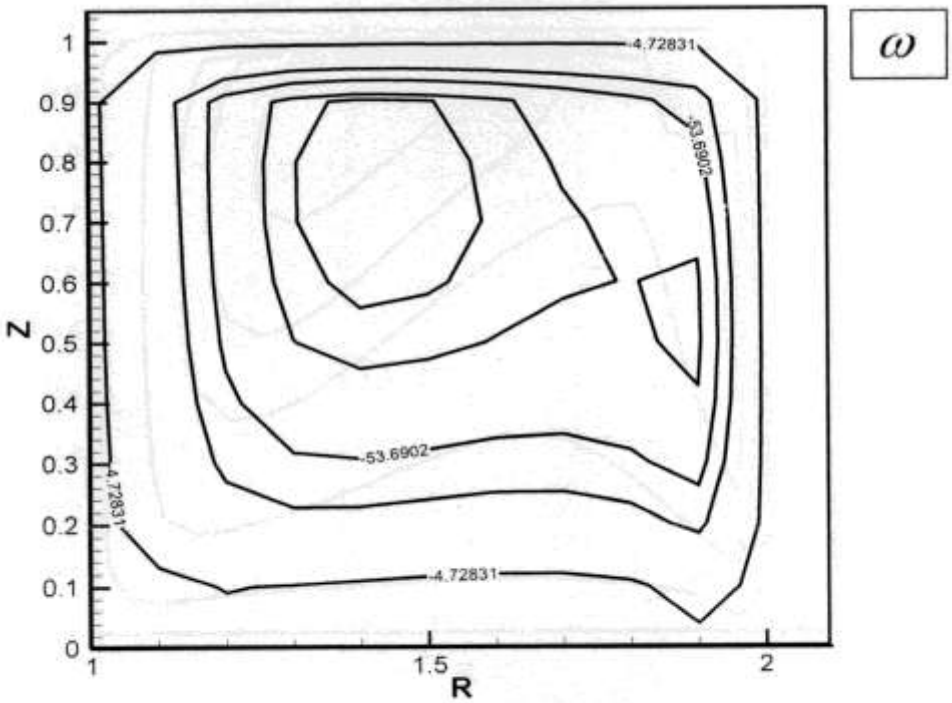

$Ra_d = 10^3$

Fig. (18a) Steady State Vorticity Lines for $Ra_d = 10^3$

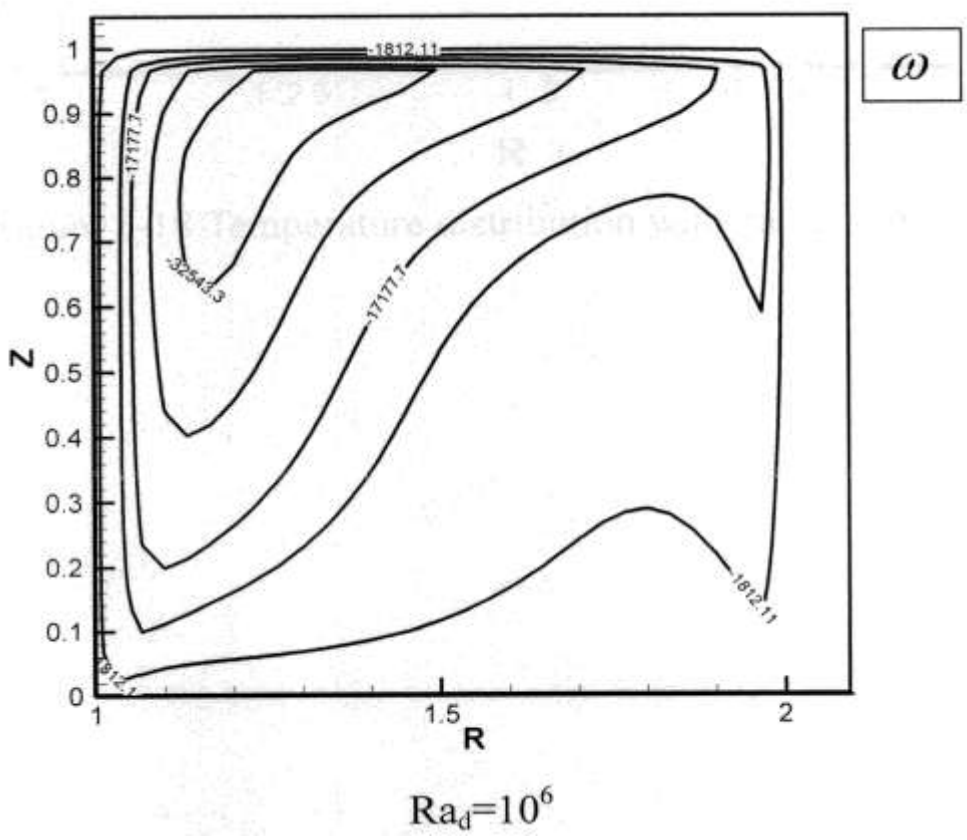

Fig. (18b) Steady State Vorticity Lines for $Ra_d = 10^6$

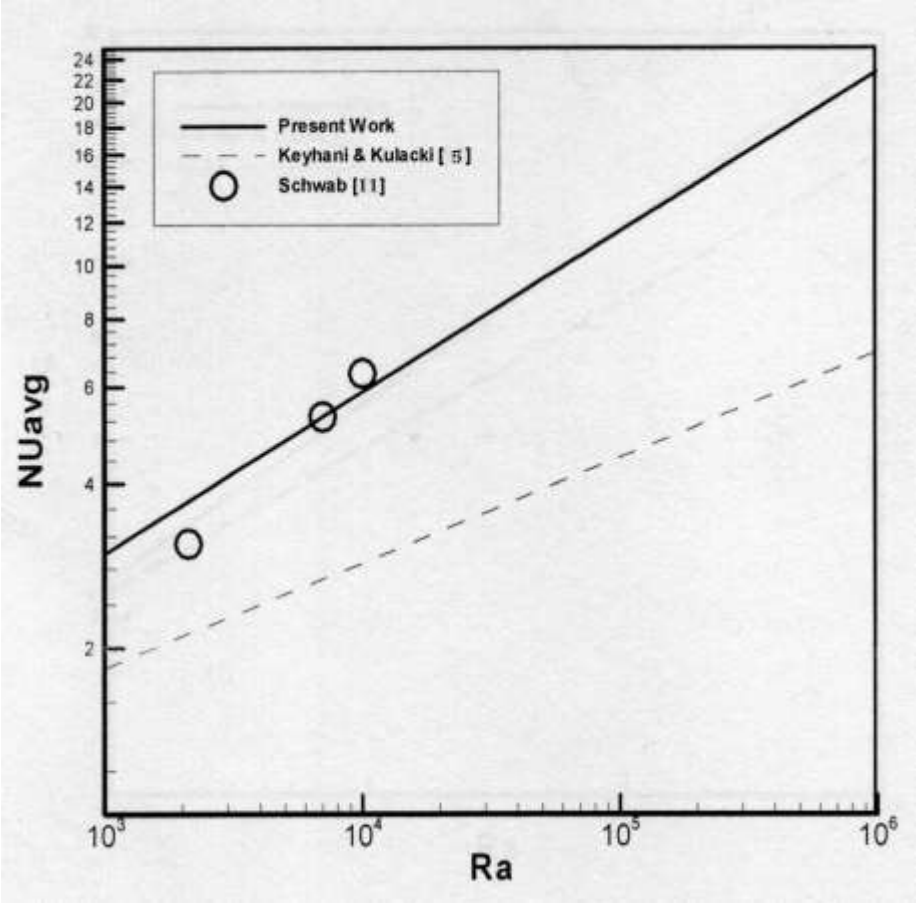

Fig. (19) Comparison between Present Work and Keyhani [5] and Schwab [11]

CONCLUSIONS

The natural convection of a mass of water contained between two concentric cylinders has been investigated numerically.

The results obtained in the present study may be summarized as follows:

1. The basic operation for heat transfer is conduction for ($Ra_d \leq 10^3$) and convection for ($Ra_d > 10^3$).
2. For the unsteady state the streamlines shows a single cell form except at ($Ra_d = 10^5$) where it shows a bicellular form.
3. The time of reaching steady state decreasing with increase of Ra_d as shown in **Fig. (15)** because the increasing of Ra_d cause an increase of liquid acceleration according to buoyancy force increasing.
4. **Fig. (17)** shows that the heat transfer operation can be divided into three regions, the first is that of heat transfer by conduction which extended to ($Ra_d=10^3$) where ($\tilde{N}u_i = 3$) and it is considered to be the start of convection region. The second region is transition region until plume region is appeared and it's ranged is ($10^3 \leq Ra_d \leq 10^4$). Third region is the plume region where ($Ra_d \geq 10^5$).

REFERENCES

Akbar Hessami, M. A., Pollard, A., Rowe, R. D., and Ruth, D. W., (1985), "A study of free convection heat transfer in horizontal annulus with a large radii ratio", ASME J. of Heat Transfer, Vol. 107, PP. 603-609.

Boyd, R., (1983), "A unified theory for correlating steady laminar natural convection heat transfer data for horizontal annuli", ASME J. of heat transfer, Vol. 105, PP. 1545-1548.

Charrier-Mojtabi, M. C., Mojtabi, A. and Caltaglrone, J. P., (1979), "Numerical solution of flow due to natural convection in horizontal cylindrical annulus", ASME J. of heat transfer, Vol. 101, PP. 171-173.

Date, A. W., (1986), "Numerical prediction of natural convection heat transfer in horizontal annulus", Int. J. of Heat and Mass Transfer, Vol. 29, PP. 1457-1464.

Keyhani M., Kulacki F. A. and Christensen R. N., (1983), "Free convection in vertical annulus with constant heat flux on inner wall", ASME J. of Heat Transfer, Vol. 105, PP. 454-459.

Kubair, V. B., and Simha, C. R. V., (1982), "Free convection heat transfer to mercury in vertical annulus", Int. J. of Heat and Mass Transfer, Vol. 25, No. 3, PP. 399-402.

Kuhen, T. H., and Golstein, R.J. (1976), "An experimental and theoretical study of natural convection in the annulus between horizontal concentric cylinders", J. of Fluid Mechanics, Vol. 74, Part 4, PP. 695-699.

Kuhen, T. H., and Golstein, R.J. (1980), "A parametric study of Prandtl number and diameter ratio effects on natural convection heat transfer in horizontal cylindrical annuli", Trans. of ASME, Vol. 102, PP. 768-770.

Lee, J. H., and Lee, T. S., (1981), "Natural convection in annuli between horizontal confocal elliptic cylinders", Int. J. of Heat and Mass Transfer, Vol. 24, No. 10, PP. 1734-1742.

Prasad, V. and Kulacki, F. A., (1985), "Free convection heat transfer liquid filled vertical annulus", ASME J. of Heat Transfer, Vol. 107, PP. 596-602.

Schwab, T. H., and De Witt, K. J., (1970), "Numerical investigation of free convection between two vertical coaxial cylinders", AICHE J., Vol. 16, PP. 1005-1010.

Shue, C., Xue, H. and Zhu, Y. D., (2001), "Numerical study of natural convection in an eccentric annulus between a square outer cylinder and circular inner cylinder using DQ method", Int. J. of Heat and Mass Transfer, Vol. 44, PP. 3321-3333.

NOMENCLATURE

Symbols	Description	Units
As	Dimensionless aspect ratio $As = \iota / (r_o - r_i)$	
g	Acceleration of gravity	m^2/sec
L	Cylinder length	m
M	Nodes number in r-direction	
N	Nodes number in z-direction	
$\tilde{N}u_i$	Average Nusselt number $\tilde{N}u_i = h (r_o - r_i)/k$	
Pr	Prandtl number $Pr = \nu/\alpha$	
R	Dimensionless radial direction $R = r/(r_o - r_i)$	
Ra_d	Rayleigh number $Ra_d = Pr\ (g\beta(T_i - T_o)\ (r_o - r_i)^3/\nu^2)$	
r_i, r_o	Inner and outer radius	m
T_M	Dimensionless time $T_M = \alpha\ t / (r_o - r_i)^2$	
t	Time	sec
T_f	Film temperature $T_f = (T_i + T_o)/2$	K
U	Dimensionless radial velocity $U = u\ (r_o - r_i)/\alpha$	
u	Radial velocity	m/sec
V	Dimensionless vertical velocity $V = v\ (r_o - r_i)/\alpha$	
v	Vertical velocity	m/sec
Z	Dimensionless vertical direction $Z = z / (r_o - r_i)$	
z	Gap width $z = (r_o - r_i)$	m

GREEK SYMBOLS

Symbols	Description	Units
ω	Dimensionless vorticity	
ψ	Dimensionless stream function	
ε	Error ratio	
Θ	Dimensionless temperature $\Theta = (T - T_o) / (T_i - T_o)$	
α	Thermal diffusivity	m^2/sec
β	Volume coefficient of expansion $\beta = 1/T_f$	1/K
ν	Kinematics' viscosity	m^2/sec